The EPMA, LA-ICP-MS and ICP-OES study of corrosion of structural materials for a nuclear reactor cooling circuit by molten fluoride salt treatment†

T. Vaculovic,[a] P. Sulovsky,[b] J. Machat,[a] V. Otruba,[a] O. Matal,[c] T. Simo,[c] Ch. Latkoczy,[d] D. Günther[d] and V. Kanicky*[a]

Received 24th July 2008, Accepted 9th March 2009
First published as an Advance Article on the web 26th March 2009
DOI: 10.1039/b812766b

Electron probe microanalysis (EPMA), inductively coupled plasma atomic emission spectrometry (ICP-OES), and laser ablation inductively coupled plasma mass spectrometry (LA-ICP-MS) were applied to study the interaction of molten LiF-NaF salt mixtures with candidate structural materials (alloys) for a nuclear reactor-transmutor cooling circuit. The corrosion of test ampoules and inserted test specimens made of structural materials was brought about by the action of molten LiF-NaF coolant at 680 °C and its extent and character were examined in dependence on the time of exposure. The material corrosion changes were studied by mapping the sections of ampoule walls and inserted specimen surfaces with EPMA, whereas LA-ICP-MS was employed for linear scanning the salt/ampoule wall boundary. Corrosion-released structural material, dissolved in solidified molten salt, was analyzed by ICP-OES after the salt dissolution. The melt activity was proved to induce a surficial modification of a structural material up to the depth of 15–50 μm, which was associated with the coolant contamination. The X-ray maps by EPMA with its 1-μm lateral resolution revealed compositional changes in alloys, such as regular depletion of Cr to the depth of 10–25 μm. While the lateral resolution of LA-ICP-MS with the applied laser spot diameter of 25 μm was not exactly adequate to dimensions of the corroded regions and, consequently, yielded less information in comparison with EPMA, this technique was quite sufficient for the monitoring of the presence of alloy constituents in an adhered salt layer. It was concluded that: *i)* the EPMA study, involving semi-quantitative elemental mapping/content profiling and detailed spot quantitative analyses makes it possible to obtain quantitative assessment of the corrosion process; *ii)* LA-ICP-MS profiles can be converted from signal domain to elemental contents on a semi-quantitative level when applying signal normalization to the total sum of signals.

1. Introduction

Nowadays, in some countries the spent nuclear fuel from commercial power reactors is accumulated at first in temporary repositories and later, considered as nuclear waste, deposited in a permanent underground repository. In other countries, reprocessing of the spent fuel is carried out to separate uranium and plutonium and produces mixed oxide fuel for power reactors. In the Generation IV of power reactors, molten salt reactors (MSR) and partitioning and transmutation methods are considered, amongst others, with the aim of utilizing fissible actinides from the nuclear spent fuel and minimizing volume and radiotoxicity of wastes for underground repositories. In the MSRs, molten fluoride salts (*e.g.* $LiF\text{-}BeF_2$, $NaBF_4\text{-}NaF$)[1] are considered, amongst others, as coolants.

Molten fluoride salts at 500 °C represent a considerably invasive and corrosive media for the material of piping and other circuit parts. It is known that fusion with alkali fluorides is used in chemical analysis for the decomposition of resistant materials, *e.g.* minerals and rocks.[2] Similarly, fluoride coolant attacks also to some extent corrosion-resistant materials of the heat exchanger circuit.[3] Consequently, besides mechanical and thermal influence of molten fluoride salts it is important to investigate their chemical effect on the constructional material.

Corrosion of the piping inner surface and composition of the fluoride in contact with the piping needs to be studied in relation both to the construction material type, and the coolant composition, as well as to the duration of the melt-exchanger contact, melt temperature and some other conditions. For the study of corrosion processes, methods of local surface elemental analysis were employed, involving glow discharge with optical emission detection (GD-OES),[4] electron probe X-ray microanalysis (EPMA),[5] atomic force microscopy[6] and scanning electron microscopy (SEM).[6,7] Changes in coolant composition, including the main constituents (*e.g.* F^-, Li^+, Na^+, K^+) as well as elements released from the construction material by corrosion

[a]*Laboratory of Atomic Spectrochemistry, Faculty of Science, Masaryk University, Kotlarska 2, 611 37 Brno, Czech Republic. E-mail: viktork@chemi.muni.cz*
[b]*Laboratory of Electron Microscopy and Microanalysis, Faculty of Science, Masaryk University, Kotlarska 2, 611 37 Brno, Czech Republic*
[c]*Energovyzkum, Ltd., Bozetechova 17, 612 00 Brno, Czech Republic*
[d]*Laboratory of Inorganic Chemistry, ETH Zurich, Wolfgang-Pauli Strasse 10, 8093 Zurich, Switzerland*

† This article is dedicated to Professor Jean-Michel Mermet, in recognition of his contributions to the field of atomic spectrometry.

(particularly Cr, Mo, Ni and Fe) need to be monitored—at first during optimization of a fluoride mixture composition and selection of a construction material type, and later for the routine operation checking.

For the analysis of fresh and used fluoride salts, atomic spectrometry methods might be appropriate, such as atomic absorption spectrometry (AAS),[8] optical emission spectrometry with inductively coupled plasma (ICP-OES).[9] Unlike local surface analysis, which is indispensable for the characterization of material changes at the boundary between the coolant and the piping, determination of contaminants in solidified fluoride coolant requires representative sampling of sufficient amount of salt due to expected inhomogeneous distribution of corrosion products. Such a sample is dissolved in (acidified) aqueous medium and analyzed by using flame AAS or ICP-OES/MS with pneumatic nebulization of the solution.[9]

The aim of this work is to evaluate the applicability and performance of selected analytical techniques for characterization of the corrosive action of fluoride (LiF-NaF) melts at temperatures above 500 °C on candidate structural materials when selecting the most resistant metal or alloy. A coolant based on a binary mixture of fluorides has been selected and included in optimization experiments designed for realization of a secondary circuit that would be used in a future transmutor. This study is applicable generally to heat exchangers that use corrosive media for heat exchange/transfer.

Besides EPMA and SEM, ICP-MS coupled with laser ablation (LA) as a means of local solid sampling was employed for the inspection of boundary alloy–solidified coolant. Unlike EPMA and SEM, which are considered routine techniques for surface elemental analysis, LA-ICP-MS has only been used very rarely so far for acquisition of elemental distribution across the boundary of this kind and therefore, it presents a novelty.[10]

The advantage of LA-ICP-MS in comparison with EPMA might consist in faster analysis and in its capability to detect lithium in corroded structural material. As the diameter of the focused laser beam is of the order of tens of micrometers while the electron beam of EPMA has typical diameter of 1 micrometer, a single line scan with LA-ICP-MS would bring information on compositional changes of a sufficiently representative area of the material section within a shorter time in comparison with EPMA, which requires the use of a raster scan for the same area. On the other hand, EPMA has excellent lateral resolution which it uses to possibly detect small material defects. The technique of LA-ICP-MS is operated at atmospheric pressure whereas EPMA operates at vacuum conditions. Degasification of porous material and evacuation of the EPMA working space needs also some time while LA-ICP-MS requires only a few seconds for ablation cell purging with the working gas.

The technique of GD-OES makes it possible to perform depth profiling perpendicularly to the corroded surface. A depth profile with a good depth resolution, which is averaged and smoothed over the sputtered area, can be obtained up to tens or hundreds of micrometers in depth. However, lateral resolution (discharge diameter of the order of mm) is not sufficient in the case of laterally inhomogeneous surfaces. However, the resulting depth profile is averaged from a large sputtered area and small material defects are not detectable. In depth profiling of corrosion layers the technique of GD-OES presents advantage over possible LA-ICP-MS depth profiling when we are not interested in lateral resolution. In contrast to LA-ICP-MS, GD-OES is capable of detecting and determining oxygen in the corroded layer, which posesses crucial information for nuclear technology development.

Concerning the corroded sample section imaging, the best results are obtained with SEM, which is ideally complementary to GD-OES depth profiling.

Consequently, LA-ICP-MS might be complementary to EPMA and comparable with GD-OES with the above limitations.

As far as the ICP-OES solution analysis of fluoride salts is concerned, the chemical reactivity of fluoride ions complicates the application of the current instrumental equipment due to corrosion of glass and quartz parts of the ICP spectrometer. Usually, a spectrometer with standard sample introduction equipment is not adapted for nebulization of sample solutions with a high content of fluorides and therefore, it was necessary to replace glass parts with components made of resistant materials, such as PFA or Teflon®.[9]

2. Experimental

Inconel (A 686) and stainless steel 1.4571 were tested as candidate materials for the construction of a reactor secondary cooling circuit. Nickel and iron are base constituents of Inconel A 686 and stainless steel 1.4571, respectively. The composition of candidate materials is given in Table 1.

Corrosion by the action of the fluoride salt mixture with the molar composition of 60% LiF and 40% NaF was studied in this work. Of the whole fluoride salt family intended for heat exchange and transfer, this candidate cooling medium was chosen for its relatively high melting temperature of 655 °C. The corrosion tests were performed in ampoules[11,12] (height 185 mm, inner diameter 21.3 mm, wall thickness 2 mm), made of candidate structural materials and filled with a mixture of LiF and NaF. Ampoules were exposed to a constant temperature of 680 °C for 380 and 1000 hours, respectively. After cooling down, the ampoule with solidified melt was cut along its axis. The melt was then ground in a ball mill. Powdered material was further processed for ICP-OES solution analysis and for titrimetric determination of fluorides.[9] The precipitation titrimetric method based on reaction of fluoride and thorium(IV) nitrate solution was applied for quantification of fluoride content. Glycine–perchloric acid–sodium perchlorate buffer was applied for adjusting the pH value to 3.4 while ascorbic acid served as a masking agent for Fe(III), otherwise interfering with indication of equivalence. Methylthymol blue indicates equivalence and changes from blue [complex indicator–Th(IV)] to yellow (free indicator).[13]

Table 1 Composition of candidate materials for construction of a transmutor secondary cooling circuit obtained by EPMA on the examined samples

	Elemental content (% m/m)										
Material	Si	P	Mn	Co	W	Fe	S	Ti	Mo	Cr	Ni	Total
1.4571	1.0	0.045	2.0	—	—	64.3	0.03	0.8	2.25	17.5	12	99.93
Inconel	0.05	0.001	0.25	0.04	3.83	0.32	0.001	0.11	16	20.26	59.1	99.96

Annular pieces of ampoule cut with a diamond saw were further sectioned to obtain cuts perpendicular to the ampoule wall. These were embedded into epoxy resin (Araldite) disks and lapped and polished with diamond pastes for EPMA and LA-ICP-MS measurements.

Electron probe microanalysis was performed with an SX100 microprobe (CAMECA, France). The acceleration voltage was set on 15 kV. The analysis spot size was 1 μm. The standardization was checked for interferences and cross-checked with a stainless steel standard SRM 460b (SPI). The acquired quantitative data were corrected using the modified ZAF method (PhiRoZet, CAMECA).

Instrumentation for LA-ICP-MS consists of a laser ablation system LSX 500 (Cetac, Omaha, USA) and an ICP-MS spectrometer Element2 (Thermo Electron, Bremen, Germany). Optimized parameters of the ICP source and the sector field MS are summarized in Table 2. A commercial Q-switched Nd:YAG laser ablation device is designed for operation at the 4th harmonic frequency which corresponds to the wavelength of 266 nm. The ablation device is equipped with programmable XYZ-stages which makes it possible to set the required XY-position on the target surface and/or to move the sample along a programmed trajectory during ablation. Optimization of the LA-ICP-MS facility (gas flow rates, sampling depth, electrostatic lenses voltages of the MS) was performed with the glass reference material NIST SRM 612 in respect to maximum S/N ratio and minimum oxide formation (ThO^+/Th^+ count ratio 0.2%, U^+/Th^+ count ratio 1.1%).[14] A single line scan perpendicular to the alloy surface was used for LA-ICP-MS measurements with a 25 μm laser spot diameter.

For quantification purposes a normalization method which uses a total sum of signals of isotopes was employed.[10] The blank-corrected isotope signal was abundance-corrected to obtain the elemental signals. Particular elemental signals were normalized to the sum of all element signals to obtain elemental content. ICP-MS signals were measured for all elements shown in Table 1 and for Li and Na, which are present in molten fluoride salts. The fluorine signal was calculated as the sum of the Li and Na signals.

Analysis of solutions was accomplished by means of a Jobin-Yvon 170 Ultrace ICP spectrometer (JY-Horiba, Longjumeau, France), equipped with a poly- and monochromator. The standard glass sample introduction system (Meinhard concentric nebulizer and cyclonic spray chamber) was replaced with sample introduction system for fluoride solutions, which consisted of the PFA cross-flow nebulizer with solution capillary made of Pt and a spray chamber made of PFA. Matrix-matched calibration solutions were used for determination of the content of corrosion products in molten fluoride salts.

Table 2 ICP-MS operating conditions used for laser ablation study of elemental content profiles within the salt layer on the ampoule wall inner surface

ICP-MS	Element2 (Thermo Electron)
rf power	1350 W
sample gas flow	0.95 l/min Ar
auxiliary gas flow	0.6 l/min Ar
cooling gas flow	15.0 l/min Ar
carrier gas flow	0.86 l/min He
m/Δm	300
sampler/skimmer cones material	Pt

3. Results and discussion

3.1. Analysis of corroded surfaces by EPMA

The **Inconel 686** test samples exposed to melt for 1000 hours show significant compositional changes at the boundary. Quantitative results of electron microprobe analyses are presented in Table 3 and corresponding modifications of surface layer are shown in Figs. 1 and 2. In the layer between 0 and 10–20 μm below the surface, nickel is enriched by one third of the original content in the intact material (Fig. 1a). Similarly, molybdenum exhibits increased content in this layer, too. Iron and cobalt are distinctly enriched in the outermost layer between 0 and 5 μm. On the other hand, chromium content drops in the same layer to less than one-fourth of its value found in the intact material and the zone depleted in Cr exhibits quite a sharp boundary with the intact material (Fig. 1b). Besides, a part of chromium released from this surficial layer reacts with oxygen dissolved in the salt melt and forms a thin, more or less continuous chromium trioxide crust. This is evident in Fig. 1b as a thin white zone where chromium content attains double the value for the intact material. Manganese exhibits similar depletion as Cr (Fig. 1c). The crust of Cr_2O_3 is evident from the BSE (back scattered electron) surface image in Fig. 2a as well as from the BSE image of polished sections in Fig. 2b. In areas where this crystalline crust is absent

Table 3 Comparison of composition of Inconel A686 exposed to molten LiF-NaF salt mixture (microgranular phase) and of unaffected zone of Inconel A686 by means of EPMA spot analyses

Inconel A686 Elements	EPMA, Elemental content (% m/m)					
	Cr	Ni	Mo	Mn	Fe	Co
Unaffected	20.7	59	16	0.3	0.09	0.01
Corroded	5.1	74	21	0.1	1.30	0.04

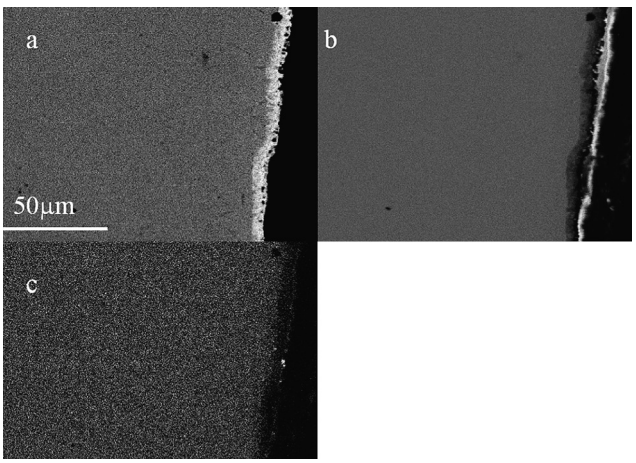

Fig. 1 X-ray elemental mapping of Inconel after 380-hours exposure to LiF-NaF at 680 °C: (a) Ni, (b) Cr, (c) Mn; lighter colour corresponds to higher content.

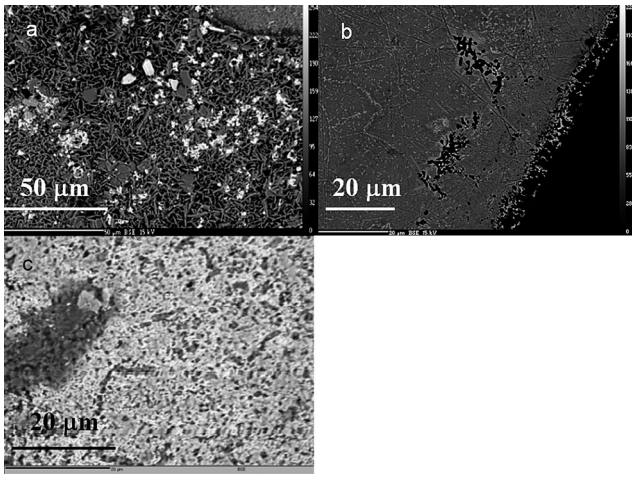

Fig. 2 Inconel after 380-hours exposure to LiF-NaF at 680 °C: (a) BSE image of surface with Cr_2O_3 crystalline salt layer (bright grey platelets) and fragments of Inconel alloy, enriched in Mo (white grains); (b) BSE image of polished section with Cr_2O_3 crust on the wall/melt boundary and voids following grain boundaries, rimmed with W, Ni-enriched material; (c) BSE image of the test body surface, area without Cr_2O_3 crust, showing pitting; in all BSE images lighter colour corresponds to higher content.

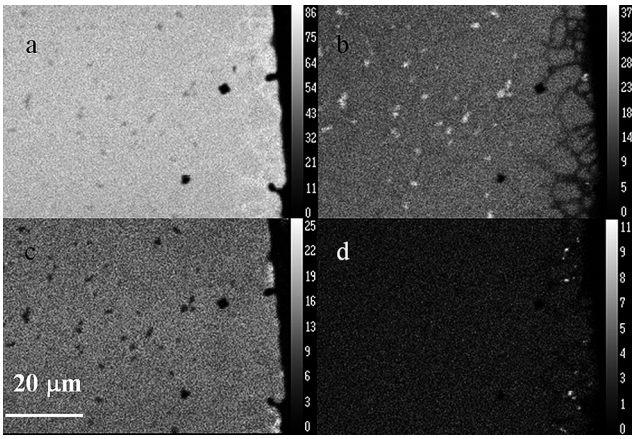

Fig. 3 X-ray elemental mapping of Stainless steel 1.4571 after 1000-hours exposure to LiF-NaF at 680 °C: (a) Fe, (b) Cr, (c) Ni, (d) Mn; lighter colour corresponds to higher content.

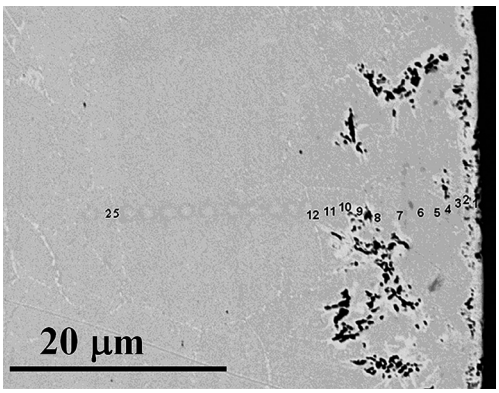

Fig. 4 Stainless steel 1.4571 after 1000-hours exposure to LiF-NaF at 680 °C: BSE image, a close-up view of the near-surface area of polished section; lighter colour corresponds to higher content.

or removed the surface appears to be punched by tiny channels or pits formed preferably at grain boundaries (Fig. 2c).These channels, which exhibit a depth less than 20 μm, are always rimmed with a narrow zone of Ni (Mo) enrichment (Fig. 2b). Based on EPMA measurements and observations it can be concluded that the corrosion of Inconel by LiF-NaF melt is characterized by two processes: *i)* diffusion and dissolution of the alloy, and *ii)* oxidation of released chromium by a trace amount of oxygen present in the argon atmosphere in the space above the fluoride melt level. The intergranular corrosion is combined with diffusional substitution of elements leached out by the melt (particularly Cr), leading to enrichment in Ni, W and Mo.

The **stainless steel** exposed for 1000 hours to the LiF-NaF melt exhibits a granular texture characterized with grains ranging from 7 to 15 μm. Lateral distribution of chromium is not homogeneous, because it contains small (1–4 μm) inclusions of a Cr/Mo-rich phase, which means weak depletion of chromium at the grain boundaries. The stainless steel 1.4571 corrosion proceeds preferentially along grain boundaries, which is evidenced by the formation of narrow etched channels (crevices) or chains of pores. The depth of these channels depends on the duration of contact with the fluoride melt and on the fact whether the static or dynamic regime is considered. The channels are rimmed with narrow Fe/Ni-enriched and Cr/Mn-depleted zones (Figs. 3a–d). The thickness of the contiguous zone of Fe/Ni enrichment is about 7 μm. The degree of enrichment of Fe, Ni, and Co represents about one fourth to one third of their original contents. Of minor and trace elements, Mn, Mo, Si and Ti are depleted in the 50-μm surficial zone. Besides the general decrease (from 2 to 1% m/m) in this zone, Mn shows also local spot enrichment up to the depth of 10 μm. The Mn-rich spots do not match the Fe/Ni enrichment zone and they are localized in some pores or parts of channels depleted in Cr (Fig. 3d). Beneath the 7-μm Fe/Ni enrichment zone the Fe/Ni enrichment continues, but it follows only some grain boundaries or chained pores (Fig. 4).

3.2. Analysis of used fluoride salt coolant

The main cationic constituents of the coolant—sodium and lithium—were determined by ICP-OES, similarly to the products of ampoule wall corrosion. Mutual non-spectral interferences of the main cationic constituents (Li, Na) are observed even when measuring the signal in the normal analytical zone. These multiplicative interferences were eliminated by using matrix-matched calibration solutions containing theoretically the same amount of both elements as analyzed samples. This precaution compensates for the Li and Na signal depression observed with solution containing at the same time both Li and Na in comparison to single-element Li, Na solutions. On the contrary, the matrix effect of fluoride ion on Na/Li signals was not observed despite a relatively high F^- concentration (500 mg/l). This can be explained by the high first ionization energy of fluorine which causes only insignificant fluorine ionization in the plasma. Hence it has only negligible impact on excitation processes in the ICP source.

Contents of corrosion products (major and medium constituents of the particular construction materials, *i.e.* Ni, Cr, Fe and Mo) were determined using matrix-matched calibration solutions. For the quantification of the overall corrosion process, the total content of corrosion products was calculated. It was found that the content of corrosion products increased with the time of exposure for both materials and it was observed that stainless steel exhibited higher corrosion rate in comparison to Inconel (Table 4). The sum of corrosion products of the stainless steel was close to 0.6% m/m after 1000 h of exposure. In the case of Inconel the sum of corrosion products was three times lower in comparison with stainless steel. Detailed information on the presence of individual elements of corroded structural material in exposed salt mixture was published in ref. 9.

3.5. Qualitative profiling of metal/salt boundaries by LA-ICP-MS

Compositional changes along the boundary salt layer/alloy were determined for Inconel A686 and stainless steel 1.4571 exposed to LiF-NaF mixture at 680 °C after the 380-hours and 1000-hours exposure. The samples were ablated perpendicularly to the sample surface in several areas of the sample surface. The concentration of all elements was calculated using the total sum of signal normalization method. The thickness of the affected zones is determined based on lithium and sodium contents because these elements are not present in the original candidate material and their presence is caused by molten fluoride salt treatment only. Fig. 5 represents a single line scan over Inconel A686 sample after 380-hours exposure. Compositional changes are observed in the affected zone. Nickel, molybdenum and iron are enriched in this layer in comparison with non-affected material whereas chromium and manganese are depleted in this zone. Elemental contents of corroded and non-affected materials are shown in Table 5. Elemental content is not homogeneous in the corroded layer hence the concentration interval is used in Table 5. Inconel A686 exposed to 1000-hours molten salt treatment shows similar behavior; same elements are enriched and depleted, respectively. The main difference consists in the thickness of the affected zone (Table 6). Longer molten salt treatment causes larger damage of the sample surface; 90 μm for 380 hours and 120 μm for 1000 hours.

Stainless steel exposed to molten fluoride salt treatment during 1000 hours shows great inhomogeneity in lateral elemental distribution, which is evident in Table 7. First the line scan shows a large depletion of Fe, Ni and Mo in the corroded layer in comparison with non-affected material. The content of Cr and

Table 4 Total content of corrosion products in the salt mixture after 380-h and 1000-h exposure at 680 °C determined by means of ICP-OES

Sample	Inconel A686		Steel 1.4571	
Exposure time [h]	380	1000	380	1000
Sum of corrosion products (% m/m)	0.12	0.19	0.23	0.63

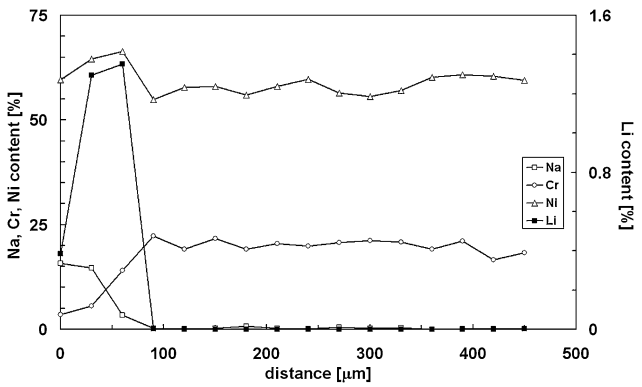

Fig. 5 The LA-ICP-MS single-line scan of Inconel after 380-hours exposure to LiF-NaF at 680 °C.

Table 5 Composition changes on Inconel A686 induced by the action of molten LiF-NaF salt mixture at 680 °C for 380 h and 1000 hours, found by means of LA-ICP-MS measurements performed in two affected areas of a sample, and for comparison in adjacent unaffected regions

	Inconel A686 sample			
	Time of exposure (h)			
	380		1000	
Element	Corroded (% m/m)	Unaffected (% m/m)	Corroded (% m/m)	Unaffected (% m/m)
Li	0.42–1.40	—	0.22–0.96	—
Na	0.36–15.8	—	1.05–9.13	—
Cr	3.51–14.1	20.0	1.71–13.3	20.5
Mn	0.04–0.10	0.40	0.03–0.43	0.32
Fe	0.18–0.70	0.05	0.11–0.55	0.05
Ni	69.7–76.4	60.2	68.3–74.6	59.9
Mo	18.3–19.5	15.4	16.3–18.6	15.6

Table 6 Thickness of affected zone of the candidate materials after 380 h and 1000 h exposure at 680 °C

Material	Inconel A686		Steel 1.4571	
Exposure time [h]	380	1000	380	1000
Affected zone thickness [μm]	90	120	125	240

Table 7 Composition changes on stainless steel 1.4571 induced by the action of molten LiF-NaF salt mixture at 680 °C for 1000 hours, found by means of LA-ICP-MS measurements performed in two affected areas of a sample, and for comparison in adjacent unaffected regions

	Stainless steel 1.4571sample			
	Analyzed area 1		Analyzed area 2	
Element	Corroded (% m/m)	Unaffected (% m/m)	Corroded (% m/m)	Unaffected (% m/m)
Li	0.09–1.94	—	0.24–1.57	—
Na	0.64–19.5	—	0.10–9.31	—
Cr	15.2–18.6	17.9	2.25–5.70	17.8
Mn	1.85–1.95	2.15	0.80–1.42	2.20
Fe	30.9–34.5	67.5	71.9–74.0	66.2
Ni	3.17–4.88	11.4	6.79–8.16	11.6
Mo	0.60–1.68	2.68	1.26–2.13	2.71

Mn in this layer is close to the content in the non-affected layer. A different course is observed for the line scan in the other part of the sample; Fe is enriched in this part of the corroded layer whereas Cr, Mn, Mo and Ni are depleted in this zone. However, differences are not visible in the case of the thickness of the corroded layer, which is 240 μm for both line scans. Similarly to Inconel, the duration of molten salt treatment affects the thickness of the corroded layer; which attains 125 μm for 380 hours and 240 μm for 1000 hours of treatment (Table 6).

The main advantage of LA-ICP-MS in comparison with EPMA is the possibility to detect and determine Li (Na) as constituents of molten fluoride salts, which are present on the surface of the examined material due to corrosion processes during molten fluoride salt treatment. Hence LA-ICP-MS allows more accurate determination of the thickness of the corroded layer than EPMA.

4. Conclusions

Investigation of molten LiF-NaF mixture-induced corrosion of alloys that are designed as candidate structural materials for transmutor cooling circuit construction was performed in laboratory-built test equipment. The corrosion of surfaces of test ampoules and test bodies was evaluated based on results of electron probe X-ray microanalysis. Corrosion products in used fluoride salts were determined by solution analysis with ICP-OES. An elemental content profile of the solidified salt layer/alloy boundary was also obtained by means of EPMA. The results are in accordance in previous observations,[3] stating the crucial role of chromium content in the candidate alloy. The laser ablation ICP-MS technique was used for chemical mapping of the solidified salt layer/wall sections. The latter technique offers quantitative profiles with lateral resolution suitable particularly for the salt layer description. The novelty of the results consists in a detailed description of the alloy/molten salt boundary, especially of the chemical composition of the corrosion-influenced surficial zone in the alloy and its microstructure, obtained by EPMA and LA-ICP-MS.

Acknowledgements

V. Kanicky, T. Vaculovic, O. Matal, and T. Simo acknowledge the Czech Science Foundation for support of project GA 101/08/1100. V. Kanicky acknowledges the Ministry of Education, Youth and Sports, Czech Republic for support in the framework of the project MSM0021622410. V. Otruba and T. Vaculovic acknowledge the Ministry of Education, Youth and Sports, Czech Republic for support in the framework of the project MSM0021622411. J. Machat acknowledges the Ministry of Education, Youth and Sports, Czech Republic for support in the framework of the project MSM0021622412

References

1 H. Moriyama, A. Sagara, S. Tanaka, R. W. Moir and D. K. Sze, *Fusion Eng. Des.*, 1998, **39**, 627.
2 M. Q. Li and G. L. Messing, *Thermochim. Acta*, 1984, **78**, 9.
3 C. A. C. Sequeira, *High Temperature Corrosion in Molten Salts*, Trans Tech Publications, Enfield, USA, 2003.
4 L. Martinelli, F. Balbaud-Celerier, G. Picard and G. Santarini, *Corros. Sci.*, 2008, **50**, 2549.
5 M. Suarez, S. Bellayer, M. Traisnel, W. Gonzales, D. Chicot, J. Lesage, E. S. Puchi-Cabrera and M. H. Staia, *Surf. Coat. Technol.*, 2008, **202**, 4566.
6 R. M. Pidaparti and R. R. Patel, *Mater. Lett.*, 2008, **62**, 4497.
7 A. Pardo, M. C. Merino, A. E. Coy, F. Viejo, R. Arrabal and S. Feliu, *Electrochim. Acta*, 2008, **53**, 7890.
8 M. Colognesi, O. Abollino, M. Aceto, C. Sarzanini, E. Mentasi and M. Braglia, *Analusis*, 1996, **24**, 299.
9 O. Matal, T. Šimo, L. Nesvadba, V. Dvořák, V. Kanicky and J. Machát, *Z. Naturfors. Sect. A*, 2007, **62**, 769.
10 C. Latkoczy, Y. Muller, P. Schmutz and D. Günther, *Appl. Surf. Sci.*, 2005, **252**, 127.
11 O. Matal, T. Šimo, L. Nesvadba, V. Kanicky, P. Sulovsky and J. Machat, *Proceedings of the 7th Int. Symp. on Molten Salt Chemistry and Technology*, Toulouse, 2005.
12 L. Nesvadba, T. Šimo, O. Matal, M. Vávra, J. Machát, P. Sulovsky and V. Kanicky, *5th Nicholas Meeting of the Young Generation of the Czech Nuclear Society*, Brno, 2005.
13 Anonymous, *Analyst*, 1972, **97**, 734.
14 I. Rodushkin, M. D. Axelsson, D. Malinovsky and D. C. Baxter, *J. Anal. At. Spectrom.*, 2002, **17**, 1231.

